DOI: 10.2478/sbeef-2023-0012

NUMERICAL ANALYSIS OF INDUCTIVE PROXIMITY SENSORS FOR NON-FERROUS TARGETS

MARIA-CĂTĂLINA PETRESCU, L. PETRESCU
University POLITEHNICA of Bucharest, Romania, Faculty of Electrical Engineering,
313, Splaiul Independentei, 060042, district 6, Bucharest ROMANIA,
E-mail: catalina.petrescu@upb.ro, lucian.petrescu@upb.ro

Abstract. ***Proximity sensors are devices found in many fields of activity from the automotive area to robotics and beyond. Among them, proximity sensors occupy an important place due to their low price and reliable response. They are found in a wide range of sizes and detection distances. In this work, a comparative study was carried out on two constructive solutions - one shielded and one unshielded. The response provided by the sensor was followed through a 2D FEMM analysis varying a series of parameters: the material from which the target is made, the distance between the target and the sensor, as well as its operating frequency. The results highlight the influence of these parameters by changing some quantities of a magnetic nature such as the spectrum of the magnetic flux density, the magnetic energy stored by the target, respectively the inductance of the sensor coil.***

Keywords: Numerical analysis, shielded inductive proximity sensors, unshielded inductive proximity sensors.

1. INTRODUCTION

Nowadays, proximity sensors are very common in different industrial applications: handling [1], robotics [2], automotive industry [3], smartphones [4], industrial conveyor system [5], collision detection in automotive industry [6, 7], control water flow [8]. They can detect the presence or the absence of an object with no contact. Typically, proximity sensors include photoelectric, capacitive, and inductive sensors [9].

Inductive sensors operate based on Faraday's Law. One way to state Faraday's Law is that a change in magnetic flux in the sensor's coil will induce a voltage in a nearby coil or metallic target [10]. An important property of inductive sensors is that these are cheap and reliable.

Figure 1. Examples of inductive proximity sensors shielded (a) and unshielded (b) [11].

There are many proximity sensors manufacturers on the market [11-13]. Their characteristics are similar for the same fields of use and detection distances. For example, in Table 1 the main properties for two different manufacturers are presented.

Table 1. Comparison between two shielded sensors [11, 13].

Item	Sensor 1	Sensor 2
Manufacturer	Eaton	Panasonic
Code	E57P Performance	GX-300
Catalog code	E57P-30SPN10-C2	GX-330M-A-N
Diameter	30 mm	30 mm
Output	NPN open-collector transistor	NPN open-collector transistor
Sensing range	10 mm	10 mm
Current consumption	< 10 mA	< 10 mA
Operating voltage	10 – 48 V	10 – 48 V
Temperature range	- 40 – +70 ºC	-25 – +70 ºC
Length	60.3 mm	67.7 mm

The main parts of a typical inductive sensor can be depicted in Figure 2 [14]. Close to the non-ferrous metallic target is the sensing coil with an inductivity of a few μH and a resistance of 13-18 Ω [15]. These two determinates the output frequency of the sensor due to its time constant $\tau = L/R$. The sensor itself contains an oscillator circuit and the coil from which an electromagnetic field radiates out and induces eddy currents in any nearby metallic targets. The eddy currents have the effect of attenuating the oscillations from the amplifier. This reduction in oscillations is registered as the presence of a metallic object.

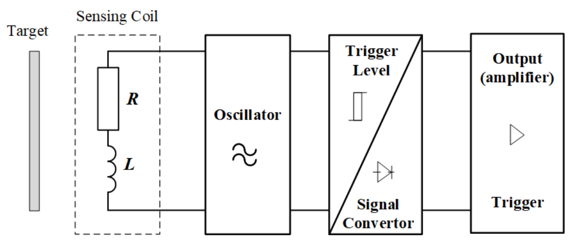

Figure 2. Schematic of an inductive proximity sensor [14].

Because only metallic targets have inductive properties, proximity inductive sensors can't be used to detect cardboard, plastic, or other non-metallic objects. However, different metals have different inductive properties and the type of metal being sensed will influence the sensing distance.

The aim of this paper is to analyze using 2D software FEMM (finite element methods in magnetic) [16]. The comparative study focused on two different sensors to find the best solution. The study will consider one shielded and one unshielded proximity inductive sensors with similar dimensions. The influence of the target materials will be considered. The dependence of the magnetic parameters with the distance between the sensor and the target and the frequency of the coil signal will be analyses in this paper also.

2. MATERIALS AND METHODS

The 2D FEMM analysis considers a quasi-stationary parallel plan problem [17, 18]. It was considered a depth of 30 mm and this way the cylindrical sensor is modeled with one with rectangular section with similar dimensions (which can be depicted in Figure 3 for shielded sensor and in Figure 4 for the unshielded one, respectively). The target has a thickness of 1 mm and a length of 40 mm. The coils are made of AWG#20 cooper (American Wire Gauge with a standard diameter of 0.812 mm) and have 96 number of turns. Each turn is supplied to 2.16 A which determines a total current of 208 A.

Each sensor is provided with a metal shell made of stainless steel with a thickness of 1 mm. The difference between the two constructive solutions consists precisely in this aspect that in the shielded model the metal shell covers the coil part, while in the unshielded model the coil is uncovered.

To highlight these data Table 1 is used.

Table 1. Initial data used in 2D simulations.

Quantity [u.m.]	Shielded Sensors	Unshielded Sensors
Length [mm]	60.3	70.3
Width [mm]	30	30
Target thickness [mm]	1	1
Coil material	AWG#20 cooper wire	AWG#20 cooper wire
Total current [A]	208	208

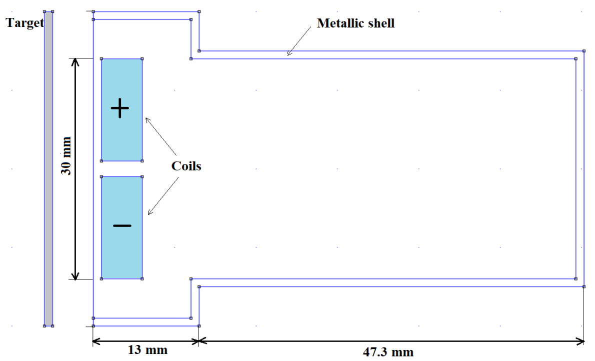

Figure 3. FEMM section of the shielded sensor.

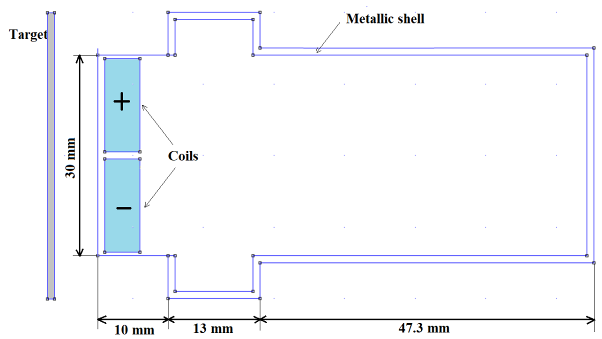

Figure 4. FEMM section of the unshielded sensor.

One of the variation parameters in this study was represented by the material from which the target is made. Thus, three linear non-ferrous metal materials were used: aluminum with an electrical conductivity of 34.45 MS/m, copper with a conductivity of 58 MS/m, respectively brass with a conductivity of 15.9 MS/m.

3. COMPARISON OF THE RESPONSE FOR DIFFERENT TARGET MATERIALS

The first part of the study was to determine how the material from which the target is made influences the response of the sensor. Initially, a constant frequency of 500 Hz was kept, and the parameters of a magnetic nature were analyzed (magnetic flux density, magnetic energy in the target and in the coil), respectively the density of the eddy currents, varying the distance between the target and the sensor from 1 to 15 mm.

Thus, in Figure 5a shows the magnetic flux density spectrum for the shielded sensor, and in Figure 5b for the unshielded one considering 5 mm between the sensor and the Al target. Keeping the same maximum limit of the spectral map, in the case of the first sensor the magnetic flux density has slightly higher values.

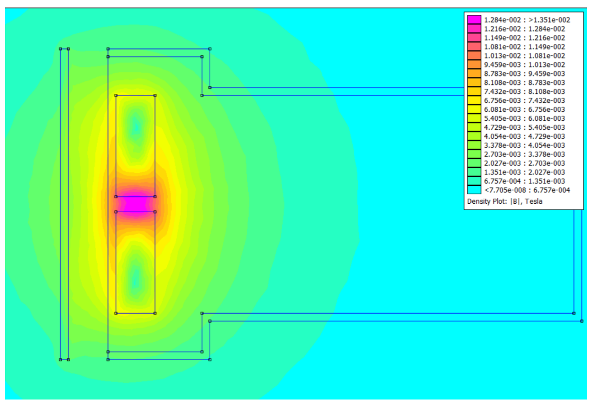

a)

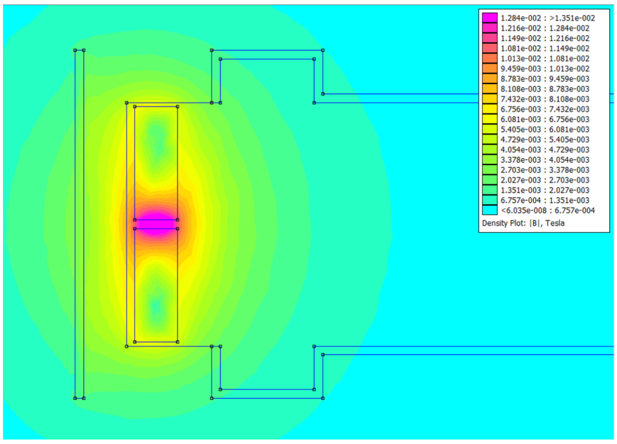

b)

Figure 5. Magnetic flux density spectrum for shielded (a) and unshielded (b) sensors with Al target.

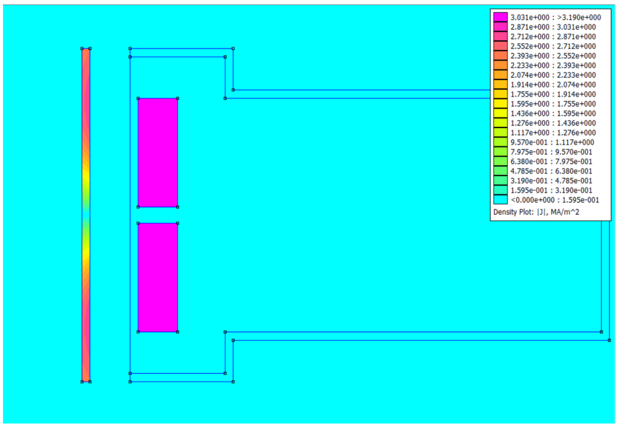

a)

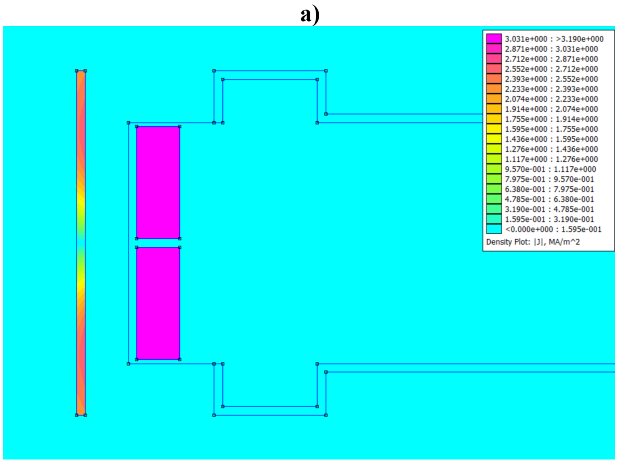

b)

Figure 6. Current density spectrum for shielded (a) and unshielded (b) sensors with Al target.

Figure 6 represents the spectrum of the conduction electric current density emphasizing the eddy currents induced in the target for the shielded sensor (a), respectively for the unshielded one (b).

To highlight the differences, in Figure 7 depicts the variation curves of the density of eddy currents along the target made of Al, both for the shielded season (solid line) and for the unshielded season (dot line) at three distances between the target and the sensor: 1 mm, 5 mm, and 10 mm, respectively. It is found, as expected, that the response of the season is directly influenced by this parameter.

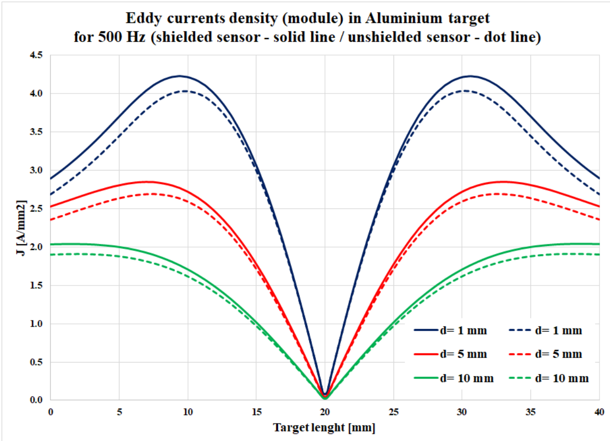

Figure 7. Eddy current in Al target for shielded / unshielded sensor for 500 Hz.

Finally, the analysis also followed the influence of the material from which the target is made. Thus, in Figure 8, a comparison was made between the density of the eddy current in the target for the three investigated materials, both for the shielded season (solid line) and for the unshielded season (dot line). The distance between the target and the sensor was kept constant (5 mm).

In Table 2 are presented the maximum value for the eddy currents density induced in the aluminum target.

Table 2. Maximum values for the eddy currents density considering the distance between the sensor and Al target.

Distance [mm]	Shielded Sensors J_{eddy} [A/mm^2]	Unshielded Sensors J_{eddy} [A/mm^2]
1	4.23	4.03
5	2.85	2.69
10	2.04	1.91
15	1.62	1.51

With the increase of the target's conductivity, the density of the eddy current increases as well, but not directly proportional to the conductivity ratio between the materials. For example, σ_{Co}/σ_{Al} = 1.68, but the mean ratio between the two curves is different region between 1.35 and 1.40. The same results were found for the comparison between copper and brass, respectively aluminum and brass.

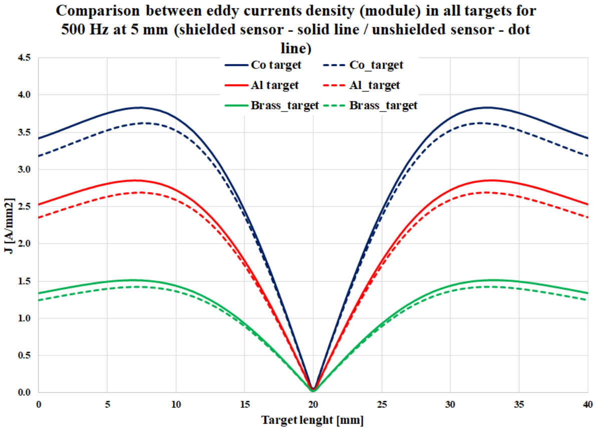

Figure 8. Eddy current in non-ferrous target for shielded / unshielded sensor for 500 Hz.

In Table 3 are presented the maximum value for the eddy currents density induced in the target, considering different materials.

Table 3. Maximum values for the eddy currents density considering different target materials for 5 mm between the sensor and the target.

Target material	Shielded Sensors J_{eddy} [A/mm^2]	Unshielded Sensors J_{eddy} [A/mm^2]
Aluminum	4.23	4.03
Cooper	3.83	3.62
Brass	1.52	1.43

4. RESPONSE DEPENDENCE ON THE TARGET DISTANCE TO THE SENSOR

As highlighted in the previous figures, the distance between the target and the sensor plays an essential role in determining its response. Thus, within this section, the comparison of various specific sizes was followed. Figure 9 shows a comparison between the magnetic energies stored by the targets in relation to the proximity between the target and the sensor: the higher the conductivity, the lower the magnetic energy.

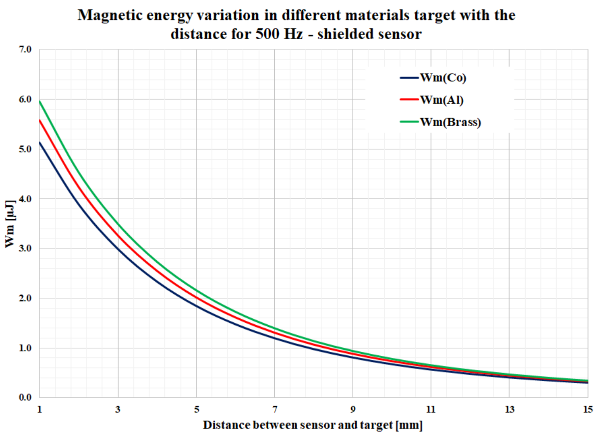

Figure 9. Comparison between magnetic energy in targets with the distance for shielded sensor.

A comparison of the curves between the shielded and the unshielded sensor was also made. Since the 6 resulting curves overlapped on various zones, in Figure 10 we chose the comparative representation only for the aluminum target. It can be observed that at the shielded sensor (solid line) the target accumulates a higher magnetic energy than in the case of the unshielded one (dot line).

The response of the sensor relative to the material of the target as well as the distance between them can be highlighted by changing the inductance of the coil. This aspect is finally translated by changing the response time. As can be seen in Figure 11, the higher the electrical conductivity of the target, the lower the inductance of the coil. Obviously, the effect is directly proportional to the proximity of the target.

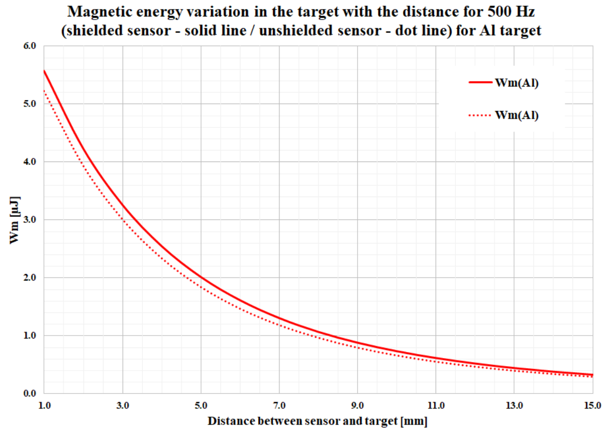

Figure 10. Comparison between magnetic energy in targets with the distance for shielded sensor and unshielded sensor for Al target.

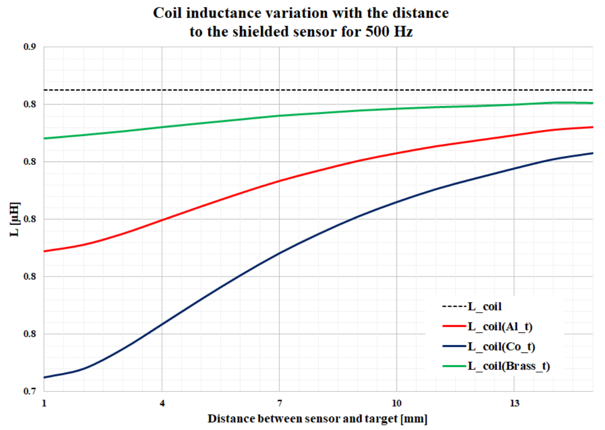

Figure 11. Comparison between variation of the inductivity of the coil for different targets.

A similar study was carried out for the unshielded sensor, with similar results. However, it is found that the reference inductance value of the unshielded sensor is superior (0.893 µH) to that of the shielded sensor (0.845 µH).

5. RESPONSE DEPENDENCES ON THE COIL SIGNAL FREQUENCY

The last part of the study focused on the analysis of the influence of the frequency of the signal in the coil for the response that the sensor offers. Thus, it started from a usage range of 500 - 2000 Hz, varying the frequency with a step of 500 Hz.

Figure 12 depicts the variation of the eddy current density in the aluminum target with increasing frequency for the screen sensor, and in Figure 13 the same curves are represented for the unshielded one.

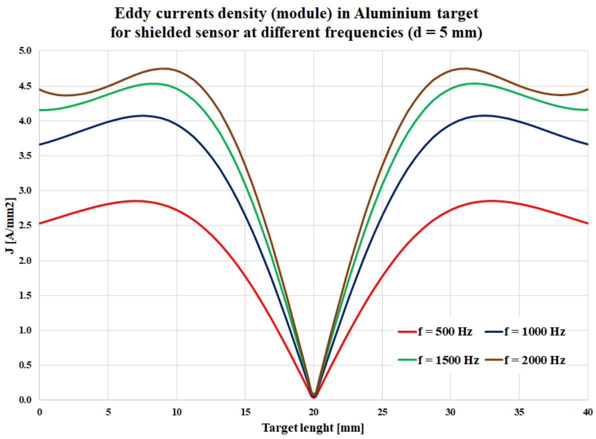

Figure 12. Eddy currents density in Al target for shielded sensor varying the frequency in the coil.

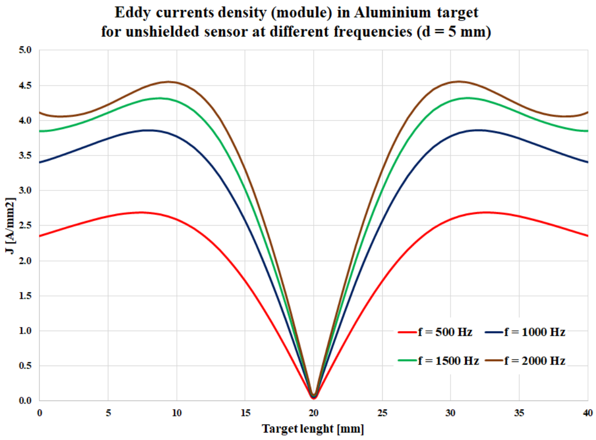

Figure 13. Eddy currents density in Al target for unshielded sensor varying the frequency in the coil.

Analyzing the previous figures, it can be seen, as expected, that as the frequency increases, the density of the eddy currents in the target increases, so we have a higher response of the sensor. It is also found that the eddy current density values are somewhat higher in the case of the shielded sensor.

In Table 4 are presented the maximum value for the eddy currents density induced in the target, considering different value of the signal frequency.

Table 4. Maximum values for the eddy currents density considering different signal frequency for 5 mm between the sensor and the Al target.

Signal Frequency [Hz]	Shielded Sensors J_{eddy} [A/mm^2]	Unshielded Sensors J_{eddy} [A/mm^2]
500	2.85	2.69
1000	4.08	3.86
1500	4.53	4.32
2000	4.74	4.55

6. CONCLUSIONS

The aim of the paper was to present a comparative numerical study on two inductive proximity sensors considering a series of parameters. Thus, using the FEMM 2D software, the variation of some quantities of a magnetic nature (magnetic flux density, magnetic energy, coil inductance) or of the eddy current density was followed. The cross-sections of two inductive sensors were used in the analysis, one shielded, the other unshielded considering dimensions and data close to the commercial ones.

The first aspect that followed was the establishment of the influence of the target material. Thus, aluminum, copper and brass targets were successively used. The results are in accordance with the material data: the higher the conductivity of the target, the higher the density of eddy currents (in fact, the sensor response). So, the highest values were obtained for the Co target.

The influence of the distance between the target and the sensor was accomplished by comparing the variation curves of the magnetic energy stored by the target, as well as the variation of the inductance of the sensor coil. In this case, as the conductivity of the target increases, the magnetic energy is reduced, so the highest value was recorded for the brass target. Also, in the case of brass, the lowest variation of the inductance of the coil was found.

The last part of the study highlighted the fact that with the increase in the frequency of the coil supply signal, the response of the sensor also increases (increase the density of the eddy currents in the target), both for the shielded and unshielded sensor.

Regardless of the varied parameters, it was found that the response of the shielded sensor is superior to the unshielded one.

7. REFERENCES

[1] F. Xia, B. Bahreyni, F. Campi, *Multi-functional capacitive proximity sensing system for industrial safety applications,* 2016 IEEE SENSORS, Orlando, FL, USA, 2016, pp. 1-3, doi: 10.1109/ICSENS.2016.7808496.

[2] S. E. Navarr, S. Mühlbacher-Karrer, H. Alagi, H. Zangl, K. Koyama, B. Hein, C. Duriez, J.R. Smith, *Proximity Perception in Human-Centered Robotics: A Survey on Sensing Systems and Applications*, IEEE Transactions on Robotics, vol. 38, no. 3, pp. 1599-1620, June 2022, doi: 10.1109/TRO.2021.3111786.

[3] C. Xing, *Perspective of Proximity Sensors on Robots Using Cross-Thought*, Highlights in Science, Engineering and Technology, vol. 32, TPCEE 2022, 2023, pp. 1-13, https://doi.org/10.54097/hset.v38i.5973.

[4] R. Moheimani, P. Hosseini, S. Mohammadi, H. Dalir, *Recent Advances on Capacitive Proximity Sensors: From Design and Materials to Creative Applications*, MDPI Journal of Carbon Research, 2022, vol. 8(2), pp. 1-19, https://doi.org/10.3390/c8020026.

[5] M. Jagiella and S. Fericean, *Miniaturized inductive sensors for industrial applications*, SENSORS, 2002 IEEE, Orlando, FL, USA, 2002, pp. 771-778 vol.2, doi: 10.1109/ICSENS.2002.1037204.

[6] S. Fericean, R. Droxler, *New Noncontacting Inductive Analog Proximity and Inductive Linear Displacement Sensors for Industrial Automation*, IEEE Sensors Journal, vol. 7 (11), pp. 1538-1545, 2007, 10.1109/JSEN.2007.908232.

[7] A. Ksentini, Z. Hadef, El-Bahi Azzag, *Management and Modeling of a Hybrid Electric Vehicle*, Scientific Bulletin of the Electrical Engineering Faculty, vol. 22 (2), 2022, pp. 18-25, https://doi.org/10.2478/sbeef-2022-0015.

[8] S. Pannala, A. Weng, I. Fischer, J. B. Siegel, Anna G. Stefanopoulou, *Low-Cost Inductive Sensor and Fixture Kit for Measuring Battery Cell Thickness Under Constant Pressure*, IFAC-PapersOnLine, Volume 55, Issue 37, 2022, Pages 712-717, https://doi.org/10.1016/j.ifacol.2022.11.266.

[9] C. W. da Silva, *Sensors and Actuators, Engineering System Instrumentation, Second Edition*, CRC Press, 2015.

[10] C Bartolettiy, R Buonanniy, L G Fantasiay, R Frullaz, W Gaggioliy and G Sacerdotiy, *The design of a proximity inductive sensor*, Meas. Sci. Technol. 9 (1998) 1180–1190.

[11] Inductive Proximity Sensors, Volume 8—Sensing Solutions CA08100010E—September 2017, Eaton.

[12] Functional Safety in Direction Detection for AGV Control Systems, Application Report | 03.2023 | AGV, https://www.pepperl-fuchs.com/global/en/classid_143.htm.

[13] Standard Type Cylindrical Inductive Proximity, GX-300 SERIES, Panasonic Industry.

[14] T. Strinic, B. Wex, G. Jungmayr, T. Stallinger, J. Frevert, M. Panholzer, *An Alternative Method for Calculating the Eddy Current Loss in the Sleeve of a Sealless Pump*, Actuators 2021, 10(4), 78; https://doi.org/10.3390/act10040078.

[15] P. Kejık, C. Kluser, R. Bischofberger, R. S. Popovic, *A low-cost inductive proximity sensor for industrial applications*, Sensors and Actuators A 110, 2004, pp. 93–97, doi: 10.1016/j.sna.2003.07.007.

[16] © FEMM Software, https://www.femm.info/wiki/HomePage.

[17] V. Solcanu, M. Gaiceanu, M. Constantinescu, G. Samoilescu, A. Sotir, *Modeling of Dispersion Magnetic Fields Developed by the Main Electromagnetic Systems Used on Military Ships*, Scientific Bulletin of the Electrical Engineering Faculty, vol. 20 (1), 2020, pp. 40-43, DOI: 10.2478/sbeef-2020-0109.

[18] V. Solcanu, M. Gaiceanu, M. Constantinescu, G. Samoilescu, A. Sotir, *Modeling of the Dispersion Magnetic Fields for the Single-Phase Transformers*, Scientific Bulletin of the Electrical Engineering Faculty, vol. 20 (1), 2020, pp. 50-55, DOI: 10.2478/sbeef-2020-0111.